Conifer Growth During Warming Hiatus in the Altay-Sayan Mountain Region, Siberia

15

Viacheslav I. Kharuk, Sergei T. Im, and Il'ya A. Petrov

Abstract

"Warming hiatus" occurred in the Altay-Sayan Mountain Region, Siberia, in c. 1997–2014. We analyzed evergreen conifer (EGC: *Pinus sibirica* du Tour and *Abies sibirica* Ledeb. mainly) stands area (satellite data) and trees (*Pinus sibirica, Larix sibirica* Ledeb.) growth response to climate variables before and during the hiatus. During the hiatus, the EGC area increased in highlands (+30%), whereas at lower elevations (<1000 m a.s.l.), the area decreased (−7%). In highlands, the EGC area changes correlated with summer air temperature mainly, whereas at lower elevations, the changes correlated with drought index SPEI. EGC mortality (Siberian pine and fir mainly) in lowland was caused by the synergy of water stress (inciting factor) and bark-beetle attacks (contributing factor). Within alpine forest–tundra ecotone (2000–2280 m), the larch growth index (GI) was limited by air temperature, whereas the Siberian pine GI was also sensitive to precipitation, root zone moisture content (RZM) and sunshine duration. Warming led to transformation of krummholz Siberian pine into vertical form, whereas larch had vertical forms before warming. Within high elevation belt (1200–2000 m), the Siberian pine growth index (GI) permanently increases since warming onset; the GI positively responded to June–July temperatures and negatively responded to moistening parameters (precipitation, root zone moisture content, and SPEI). At middle elevation, the Siberian pine GI curve has a breakpoint (c. 1983) followed by GI depression. After the breakpoint, the GI correlation with air temperature switched from positive to negative. At the same time, positive correlations between the GI and "moisture parameters" (precipitation, RZM, SPEI) increased. Under projected climate change scenario, Siberian pine will shrink its habitat at middle and low elevations with substitution by drought-resistant larch and softwoods species.

V. I. Kharuk (✉) · S. T. Im · I. A. Petrov
Sukachev Institute of Forest SB RAS, FRC Krasnoyarsk Science Center SB RAS, Krasnoyarsk, Russia

V. I. Kharuk · S. T. Im
Siberian Federal University, Krasnoyarsk, Russia

S. T. Im
Reshetnev Siberian State University of Science and Technology, Krasnoyarsk, Russia

15.1   Introduction

The effects of climate change on coniferous forests, both positive and negative, were observed throughout the boreal zone (e.g., Andregg et al. 2013; Allen et al. 2015). Conifer decline (*Picea ajanensis* Fisch., *Abies nephrolepis* (Trautv.) Maxim.) was noticed in the Russian Far East (Man'ko et al. 1998) and in Siberia (*Abies sibirica* Ledeb., *Pinus sibirica* du Tour) (Kharuk et al. 2013a, 2017b, c, 2018). Spruce (*Picea abies* L.) mortality in the European part of Russia and Eastern and Western Europe is associated with the deterioration of water condition (Chuprov 2008; Sarnatczkii 2012; Haynes et al. 2014; Kharuk et al. 2015). Along with moisture-sensitive spruce, mortality of drought-tolerant *Pinus sylvestris* L. has been observed on the southern range of this species in the Ukraine and Belarus (Luferov and Kovalishin 2017). Extensive conifer mortality has been reported in the forests of the USA and Canada (Millar and Stephenson 2015; Kolb et al. 2016). Alongside conifers, deciduous trees (*Populus tremuloides* Michx., *Betula pendula* Roth) also suffer from the increased drought (Michaelian et al. 2011; Kharuk et al. 2013b; Hogg et al. 2017). Climate warming also leads to mass insect attacks—bark-beetles, xylophages, needle-eating pests (Allen et al. 2010, 2015; Kharuk et al. 2017b, c). In particular, climate changes promote Siberian silkmoth (*Dendrolimus sibiricus* Tschetv.) northward migration (Kharuk et al. 2017d). Currently, one of the main factors of forests degradation is earlier dormant species, such as *Polygraphus proximus* Blandford which attacks have led to the mass mortality of *Abies sibirica* Ledeb. in Siberia (Krivets et al. 2015; Kharuk et al. 2017b). In the North American forests, the synergy of water stress and insects attacks resulted in tree mortality in the area of 25 million ha (Coleman et al. 2014; Millar and Stephenson 2015).

Alongside negative impacts, climate change led to the upward and northward treeline shifts (Devi et al. 2008; Kharuk et al. 2010, 2017a; Petrov et al. 2015). Warming promotes "dark needle conifer" (*Abies sibirica, Pinus sibirica, Picea obovata* Ledeb.) migration into the zone of larch dominance (Kharuk et al. 2005), and evergreen conifer (EGC) density increase in some ecoregions (He et al. 2017). These positive impacts referred to "accelerating warming" period (c. 1970s 2014 late 1990s) mainly. Meanwhile, controversial data are reported for the followed "hiatus" period, i.e., warming anomaly observed in 1998–2013, when air warming rate fell below long-term average warming rate (Hartmann et al. 2013; Medhaug et al. 2017).

This study aims at the analysis of the EGC (mainly *Pinus sibirica* and *Abies sibirica*) area dynamics in different elevational belts of the Altay-Sayan region (ASR) during warming hiatus. The ASR is one of the priority ecoregions in the Asian continent (Fig. 15.1). The mountainous terrain of the ASR shapes considerable eco-climatic gradients which make mountain forests a sensitive indicator of climate changes. These forests should experience noticeable distributional and compositional dynamics driven by changes in air temperature, water regime, and growing season length.

We hypothesized different EGC response to warming in different elevation belts with the modification effect of relief features. We are seeking the answers to the following questions: (a) What is the dynamics of the EGC area in different elevation belts? (b) How do relief features (exposure, slope steepness) modify the EGC area dynamics? (c) How did the tree growth respond to the climatic variables?

15.2   Materials and Methods

15.2.1   Study Area

The Altai-Sayan Region (Fig. 15.1) has a total area of ~85 million ha. The forested area is about 39 million ha, including ~7.7 million ha of evergreen conifers (MODIS satellite derived estimates). Mountain relief prevails on the territory with the absolute height up to 4330 m a.s.l. The main tree species are Siberian pine (*Pinus*
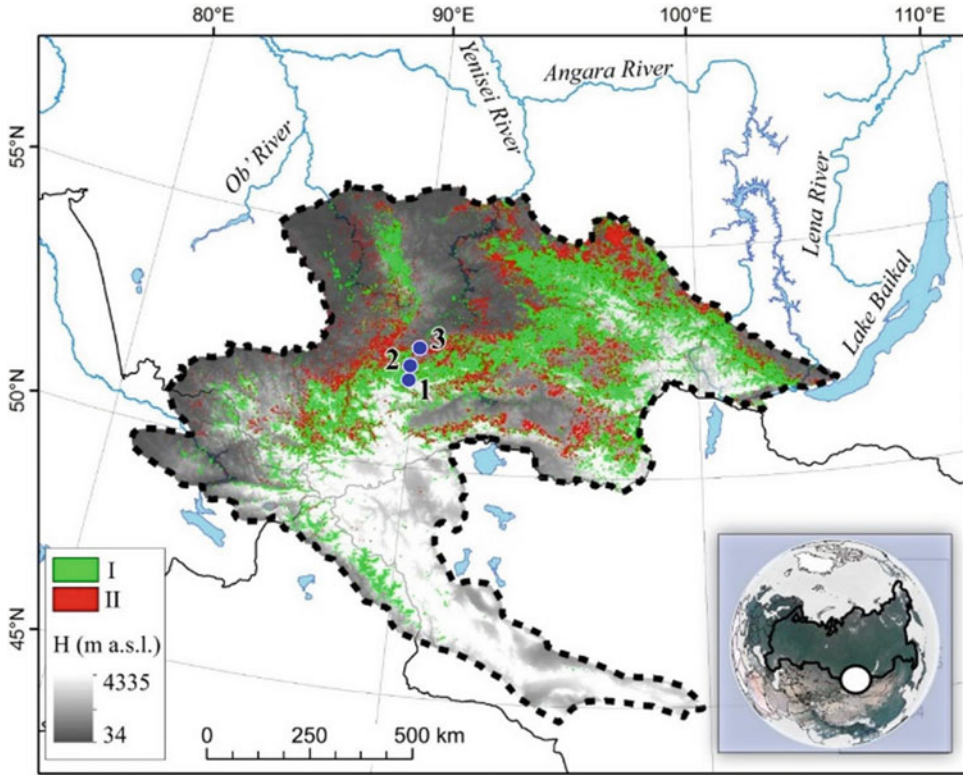
Fig. 15.1 Sketch map of the Altay-Sayan Region. Positive (*I*) and negative (*II*) trends in EGC areas are indicated by *green* and *red*, respectively. *1, 2, 3*—test sites within alpine forest–tundra ecotone, high and middle elevation belts. *H*—elevation above sea level

sibirica), fir (*Abies sibirica*), spruce (*Picea obovata*), pine (*Pinus sylvestris*), and larch (*Larix sibirica*) (Fig. 15.2).

The low elevation belt of the northern megaslope is composed by mixed forests of pine, larch, birch (*Betula sp.*), and aspen (*Populus tremula* L.). At higher elevation (800–900 m), these forests are replaced by "dark coniferous taiga" (composed by *Pinus sibirica* and *Abies sibirica*). This taiga covers elevations up to 1700–1800 m, where it gradually turns into Siberian pine or larch woodlands. Alpine tundra occupies elevations above 2000–2200 m. On the southern megaslope, the mountain forest steppe (with larch domination) prevails at elevations up to 1200–1500 m and is then replaced by the belt of mixed larch and Siberian pine forests up to 1800–2100 m.

The climate is sharply continental with cold winters and cool summers. The average temperatures are −15 °C … −18 °C in January, +10 °C … +14 °C in July (at the foothills around +19 °C … +20 °C). The amount of precipitation on the windward slopes reaches 1200–2500 mm. The averages (2000–2017) for the region temperature and rainfall were −2 °C (summer +15 °C, winter −21 °C) and 495 mm (summer—215 mm, winter—50 mm), respectively.

15.2.2   Materials

The dynamics of the EGC stand area was analyzed using MODIS products (on-ground resolution 500 m, period of 2001–2013; product MCD12Q1: https://lpdaac.usgs.gov/dataset_discovery/modis/

Fig. 15.2 High-elevation West Sayan Mountain taiga forests

modis_products_table/mcd12q1; Friedl et al. 2010). The burned areas were excluded from the analysis with the available MCD64A1 data (https://modis-fire.umd.edu). DEM GMTED2010 with on-ground resolution 250 m and elevation error 28 m (https://lta.cr.usgs.gov/GMTED2010) was used for geospatial analysis.

Dependences of the EGC area and growth index (GI) were analyzed with the main eco-climatic variables: air temperature, precipitation, vapor pressure deficit (VPD), drought index SPEI, root zone moisture content (RZM), sum of active temperatures ($t \geq +5$ °C), and growth period length (the number of days with $t \geq +5$ °C). According to Rossi et al. (2008), in cold regions, conifer cambium activity starts at temperatures of about $+4 \ldots +6$ °C. Temperature and precipitation data were drawn from the CRU TS 4.01 dataset (https://crudata.uea.ac.uk/cru/data/hrg; Harris and Jones 2017). The values of SPEI were taken from the website https://spei.csic.es (spatial resolution $0.5° \times 0.5°$). SPEI is determined by the difference between precipitation and potential evapotranspiration (Vicente-Serrano et al. 2010). The root zone moisture

content and the number of days with the specified temperature were calculated with MERRA2 data ($0.5° \times 0.625°$ resolution, https://gmao.gsfc.nasa.gov/reanalysis/MERRA-2; Gelaro et al. 2017). The wood samples for dendrochronological analysis were taken using the increment borer at "breast height" level (1.3 m) or root collar during field studies in 2014–2018.

15.2.3 Methods

The maps of EGC density trends were generated based on the MCD12Q1 maps (the differences between the average values in 2011–2013 and 2001–2003). In the specified maps, according to the IGBP classification, lands dominated by woody vegetation with a percent cover >60% are referred to evergreen forests. Along with absolute, the normalized areas A_i were assumed as the ratio of an absolute area B_i to C_i area of i-elements of relief (Kharuk et al. 2010). The analysis algorithm of the EGC maps included the following stages. (1) Creation of a burned area mask based on MCD64A1 data. (2) Filtration of

burned areas. (3) Cutting the selected fragment of the territory and transforming it into Albers equal-area projection. (4) Formation of binary layers (EGC and background). (5) Assessment of maps for the initial (2001–2003) and final (2011–2013) periods assuming that EGC pixel is registered on the maps for the initial and final periods only if it was observed simultaneously on all images of the considered period. (6) Assessment of changes in the EGC areas between the initial and final periods. (7) Calculation of area changes distribution for the relief features (elevation, exposure, slope steepness). (8) Calculation of the EGC stands spatial density for each year using the method of focal statistics with averaging within a sliding window of 5 pixels. (9) Generation of a multilayer composite covering the entire analyzed period. (10) Calculation of linear trends for each pixel. The raster of trend lines slope coefficients, the significance levels of trends, and the Pearson correlation coefficient were calculated. (11) Calculation of areas with statistically significant ($p < 0.05$) trends of the EGC density. (12) Calculation of zones with statistically significant ($p < 0.05$) trends in climate variables. (13) Calculation of trends distribution for the relief features. The algorithm is implemented using ESRI ArcGIS and Python script. In each elevation belt, test sites (TS) were established. TS description includes forest type, species composition, and number of trees, including their height and diameter, and the soil cover and soil and topographic features (direction, steepness, slope convexity/concavity, and altitude above sea level). Samples for dendrochronological analysis were randomly taken in the area of ~ 0.5 ha around TS with elevation range of about 10 m a.s.l. Within alpine forest–tundra ecotone (2280–2000 m a.s.l.), *Pinus sibirica* and *Larix sibirica* trees were sampled for the dendrochronological analysis at root collar level ($N = 20$ and $N = 13$, respectively). At high elevation (1200–2000 m) and middle (800–1200 m) elevations, *Pinus sibirica* only were sampled at dbh (1.3 m) height ($N = 28$ and $N = 46$, respectively). LINTAB 3 platform with precision 0.01 mm was used to measure wood cores (Rinn 1996). As a result, absolute

individual tree-ring chronologies (in millimeters) were obtained. TSAP and COFECHA were used to assess the quality of crossdating and measurement accuracy (Holmes 1983). To eliminate the age trend, we applied the standardization procedure that converts the time series of the annual rings width to the time series of unitless indices with a defined mean of 1.0 and a relatively constant variance (Speer 2010).

15.3   Results

15.3.1   Climate Variables Dynamics

At both low and high elevations, the "warming hiatus" was observed from c.1997 till 2014 (Fig. 15.3a, e). At high elevation, summer temperature during the hiatus increased by about +1.0 °C in comparison with the "pre-warming" period (Fig. 15.3a); the growing season increased for about three days. After the precipitation increase in 1970s–80s, a strong negative trend of minimal precipitation values has been observed (Fig. 15.3d). At low elevations, precipitation trends were not observed (Fig. 15.3b).

15.3.2   EGC Area Dynamics in the Altai-Sayan Region

The total EGC area within the ASR increased by $\sim +20\%$ during the hiatus. Meanwhile, at lower elevations (<1000 m a.s.l.), the area decreased (−7%), whereas in the highlands, the area increased by +30% (Fig. 15.4a). Negative and positive EGC trends covered 8 and 17% of the total EGC area, respectively (Fig. 15.1).

Along the elevation gradient, the EGC area changes (ΔS) switched from minus to plus at about 800 m a.s.l. (Fig. 15.4a). Maximums of ΔS decrease and increase located at 650 and 1450 m a.s.l, respectively. There is a similarity between the EGC and SPEI area distributions. Thus, forest mortality observed mainly within negative SPEI areas, whereas the EGC area increases corresponded to positive SPEI trends (Fig. 15.4b).
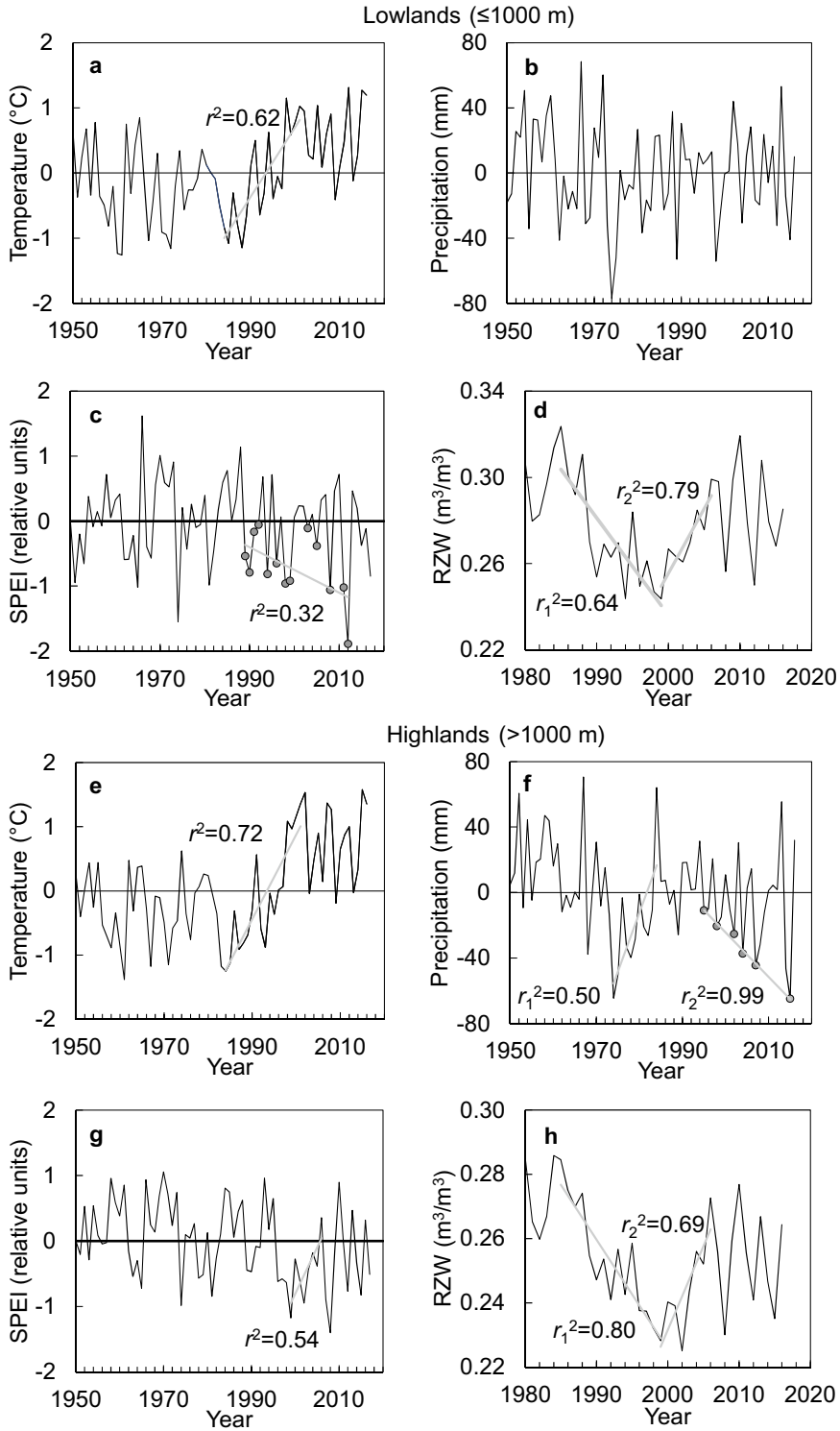
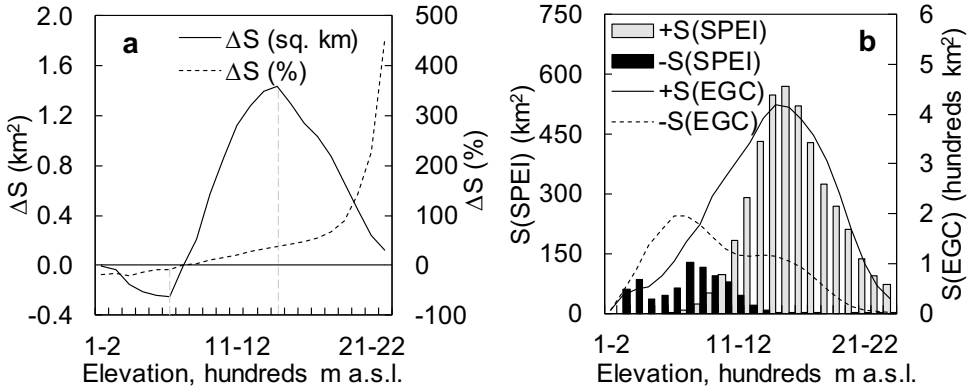Lowlands (≤1000 m)

Highlands (>1000 m)

Fig. 15.4 **a** EGC stands area changes (in square km and in %) along elevation; maximums are indicated by vertical lines; **b** EGC and drought index SPEI area trends (positive and negative) along elevation

Slope steepness and exposure have a modified impact on the EGC area changes Thus, the maximal EGC absolute area increase is located at slopes with about 10°; the relative area (in %) is increasing with slope steepness increase (Fig. 15.5a). As for exposure, the EGC area decreased on the western slopes and increased on the northern ones (Fig. 15.5b, c). In the highlands, the EGC area changes positively correlated with total summer precipitation ($r = 0.67 \pm 0.08$; $p < 0.05$) and mean summer SPEI ($r = 0.64 \pm 0.07$; $p < 0.05$). In the lowlands, the EGC area changes also positively correlated with the mean summer temperature ($r = 0.64 \pm 0.06$; $p < 0.05$), whereas correlations with SPEI are negative ($r = -0.64 \pm 0.07$; $p < 0.05$).

15.3.3 Tree Growth Index Dynamics Within Different Elevation Belts

Trees growth index dynamics was different along the elevation gradient (Fig. 15.6). Let us consider these differences with respect to climate variables.
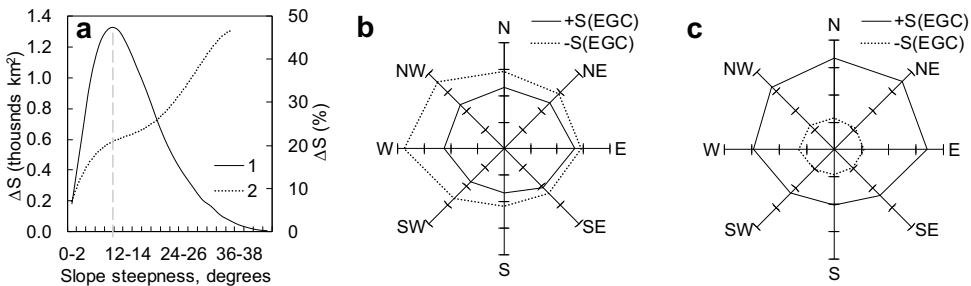

Fig. 15.5 **a** EGC area changes (ΔS) relative to slope steepness. **b**, **c** EGC area trends dependence on exposure for elevations, **b** ≤ 1000 m.a.s.l and **c** >1000 m a.s.l. respectively

15.3.3.1 Alpine Forest–Tundra Ecotone (2000–2280 m)

Alpine forest–tundra ecotone is formed by *Pinus sibirica* and *Larix sibirica* species.

Both species show a minor GI since 1970s with followed depression in the mid of 1980s and a strong GI increase since the late 1990s (Fig. 15.6a). The latter period coincided with the transformation of krummholz Siberian pine into the upright form (Fig. 15.7). Larch was growing upright during the entire observed period.

The GI of both species positively correlated with air temperature (Fig. 15.8a). The GI of Siberian pine also showed positive correlation with moisture parameters (precipitation and root zone moisture content, Fig. 15.8b, c) and negative one with sunshine duration (Fig. 15.8d). For larch, those correlations are insignificant.

15.3.3.2 High (1200–2000 m) and Middle Elevation (800–1200 m) Belts

At high and middle elevations, stands were composed by Siberian pine (dominant species) with larch as a minor component; because of that, the larch GI was not considered.

The Siberian pine GI was permanently increasing since late 1960s and that increase correlated with June temperature. Moisture parameters (precipitation, SPEI, RZM content) have a negative effect on the GI (Fig. 15.9a, b). At middle elevations, GI increase followed by growth depression with a breakpoint in c. 1983 (Fig. 15.6b, c). In late 1990s, trees split into "decliners" and "survivors" cohorts (Fig. 15.6c). At the breakpoint, the GI correlations switched from positive to negative with air temperature and from negative to positive with precipitation and SPEI; this switch was observed for both tree cohorts (except for precipitation for "survivors") (Fig. 15.9). Trees from "decliners" cohort eventually die back (Fig. 15.10).

15.3.3.3 GI Dynamics of Old-Growth Trees Within Refugium

Finally, we considered the GI dynamics of old-growth Siberian pine trees from the refugium, i.e., the zone where trees survive during LIA.

The "refugee's line" is located, dependent on relief features, at about 1800–2000 m a.s.l. (Fig. 15.11).

The elevation difference between old-growth trees and regeneration lines varied within 30–50 m. Tree establishment was poor during the period of the GI decrease (i.e., during air temperature decrease); establishment of a new generation occurred since the beginning of the GI increase (and, accordingly, to air temperature increase). The GI of old-growth trees decreased during the LIA period until the mid of the nineteenth century with following GI increase until the mid of 1940s (Fig. 15.12). Next period of the GI increase coincided with warming in 1980s. The GI of old-growth trees correlated with summer air temperature ($r^2 = 0.4$; analyzed period since the beginning of instrumental observations, 1930). No correlation with precipitation was found.

15.4 Discussion

In the Altay-Sayan Mountain Region despite of the warming hiatus, the total EGC area increased by +20%. Meanwhile, the EGC area changes were opposite in high and low elevations: in the highlands (>1000 m a.s.l.), conifer area increase was +30%, whereas in the lower elevations, area decrease observed (−7%). Similarly, observations in Southern Tibet, China, showed that while *Abies georgei* population is expanding and upper limit of this species has advanced upslope, the lowest limit has retreated upslope (Wong et al. 2010; Shen et al. 2016).

The EGC area increase in the highlands could be attributed to the higher mean air temperature (+1.0 °C) during the hiatus than in the pre-warming period (1950–1970) and longer growing season period (+3 days). The Siberian pine growth index in the highlands also permanently increased since warming onset and during the hiatus (Fig. 15.6b). Thus, during the hiatus, the EGC stand's area in the highlands increased due to improved thermal conditions on the background of sufficient precipitation. Similarly, He et al. (2017) found that evergreen conifer forest
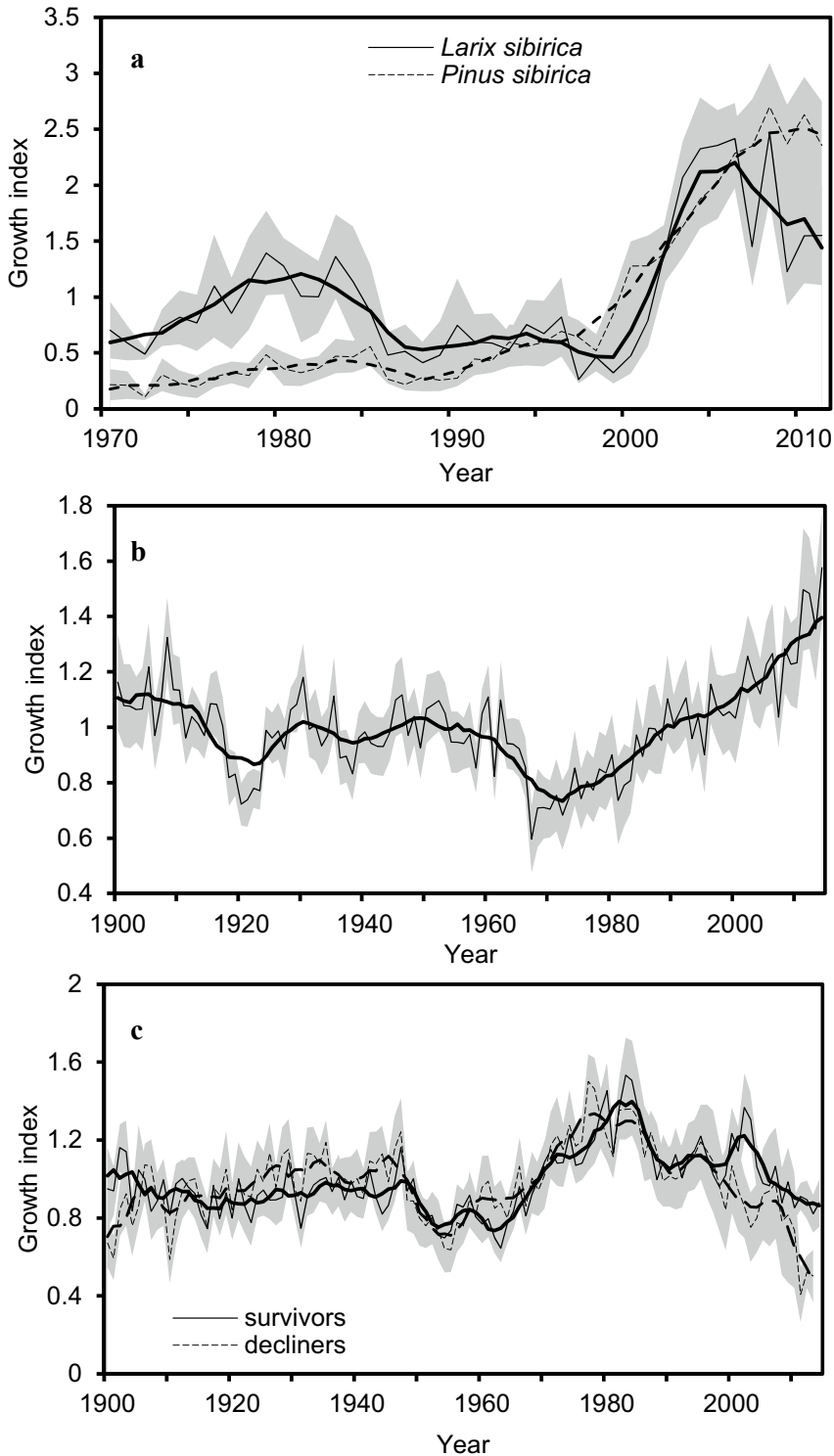
Fig. 15.6 Growth index (GI) dynamics of Siberian pine ($N = 20$) and larch ($N = 13$) in forest–tundra ecotone (**a** elevation 2030–2280 m a.s.l.), and Siberian pine at high (**b** 1200–2000 m a.s.l; $N = 28$) and middle (**c** 800– 1200 m; $N = 22$ for survivors, $N = 24$ for decliners) elevations. *Dense line*: data filtered by 11 yr. window. *Gray background*: $p > 0.05$

Fig. 15.7 *Pinus sibirica* krummholz transformed into the upright form

expansion in Western Siberia continued during the warming hiatus. Meanwhile, the highlands remained the zone of excessive moistening, which was indicated by the GI negative correlations with precipitation, root zone moisture content, and SPEI (Fig. 15.9b).

The highest relative conifer area increase observed within the alpine forest–tundra ecotone (Fig. 15.4a). On the contrary to high-elevation stands, Siberian pine within ecotone is sensitive, alongside to temperature, to the water supply, which is indicated by positive correlation with precipitation and root zone moisture content (Fig. 15.8b, c).

It is noteworthy that within adjacent high-elevation closed stands, Siberian pine growth does not depend neither on the precipitation nor the RZM content. This phenomenon is caused by poor snow accumulation due to low closure vegetation cover (Fig. 15.7). Therefore, winter

winds (with mean wind speed of about 4 m/s) blow off snow from the forest–tundra ecotone. Consequently, seedlings are located within the sites of snow accumulation, e.g., in microde-pressions, behind stones or within shrubs. That explains the GI dependence on the RZM content in the beginning of vegetation period (Fig. 15.8 c). Growth of more drought-resistant larch depended on the air temperature only. Larch is also more cold-resultant species; due to that, the larch regeneration line is located about 10 m higher in comparison with the Siberian pine one. It is worth noting that *Pinus sibirica* growth negatively correlated with sunshine duration (Feb–April), whereas larch did not (Fig. 15.8d). The effect of SD impact should be attributed to the evergreen pattern of Siberian pine: it is known that needles increased twig's surface area about 150–300 times which led to about two orders evaporation increase, Larch escaped that
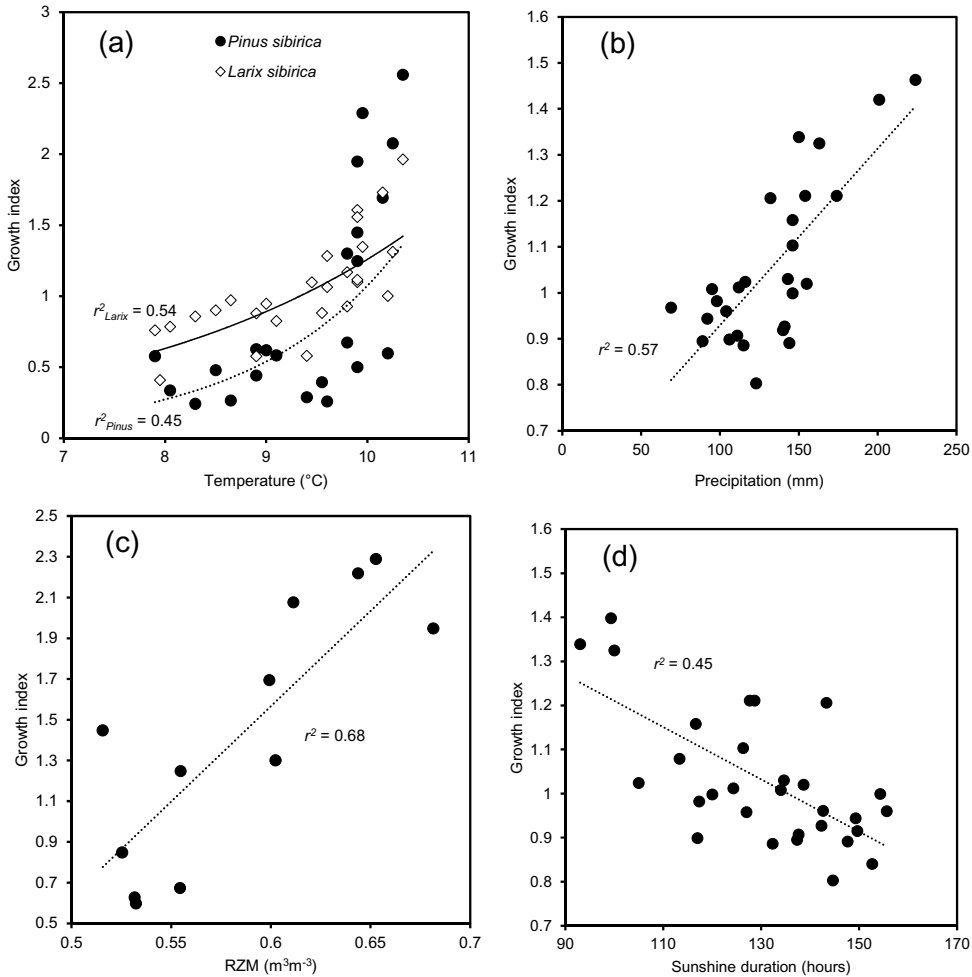
Fig. 15.8 Trees GI correlations with eco-climatic parameters within the alpine ecotone. **a** Siberian pine and larch GI correlations with air temperature (June–July 1983–2011); **b–d** Siberian pine correlations with precipitation (March–June 1982–2009), root zone moisture content (June 1996–2007) and sunshine duration (February–April 1978–2011)

effect due to its deciduous pattern. Alongside the GI increase, warming results in the fascinated phenomenon of Siberian pine krummholz transformation into upright forms (Fig. 15.7). Larch trees were vertical mainly even before warming. Due to its higher cold resistance, this species formed an upper regeneration line, whereas Siberian pine line is located about 10–20 m below. Let us note that the conifer area increase within the alpine ecotone and high elevations attributed mainly to the growth of pre-existing small trees because the observation period is too short for the area expansion due to the new trees

establishment. For example, warming-driving regeneration line upward shift estimated as 0.35–0.8 m/yr. (Kharuk et al. 2010, 2017a), or about 10–15 m for the observation period; that difference is hardly detectable by MODIS sensor.

At the middle elevation, the conifer area decrease (−7%) coincided with the moistening decrease and a strong drought episode (as indicated by SPEI values; Figs. 15.3c and 15.4).

The Siberian pine GI positive response to warming at middle elevations switched to the GI depression with a breakpoint in 1983. After the breakpoint, growth limitation by temperature
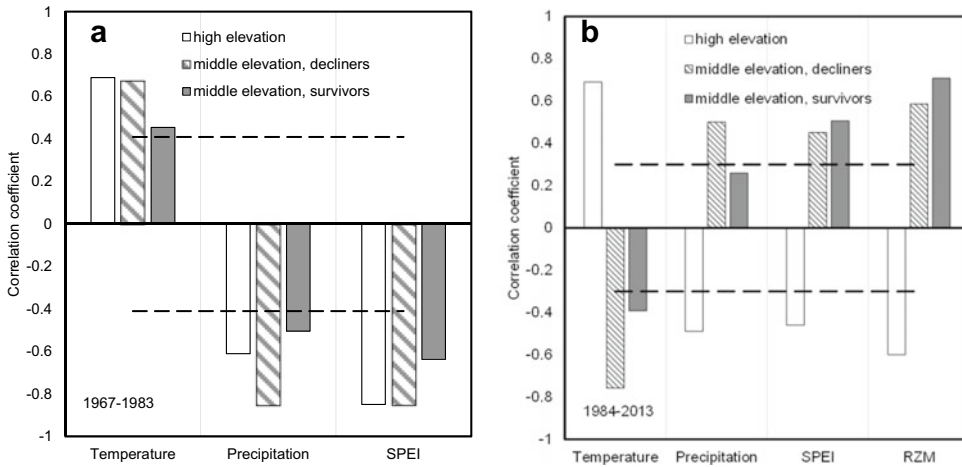
Fig. 15.9 Correlation of the GI of trees at high and middle ("survivors" and "decliners") elevations with climate variables **a** before and **b** after growth breakpoint. Variables: June temperature, May–August precipitation, May–August SPEI, July–August RZM (root zone moisture content; available since 1980). *Dashed lines* indicate $p < 0.05$ level. *Note*: SPEI decreases corresponded to drought increase

switched to limitation by moisture (Fig. 15.9). Thus, growth depression was caused by water stress via elevating air temperature. Similar switch (from temperature to moisture limitation) was described for *Pinus mugo* in high Alps (Churakova et al. 2016). Notably, the described GI decreasing pattern (Fig. 15.6c) is typical for declining stands and may precede stands mortality (Cailleret et al. 2017).

The main species that experienced mortality, as shown earlier (Kharuk et al. 2013a,2017b, c), were Siberian pine and fir (*Abies sibirica*). Meanwhile, there are no reports on the *Pinus sylvestris* or notable spruce (*Picea obovata*) mortality within the ASR, although the latter species mortality was described in Western Siberia lowlands. As for fir mortality, it was caused by synergy impact of bark-beetles and water stress (Kharuk et al. 2016). Similarly, increased water deficit together with pest attacks caused Douglas fir (*Pseudotsuga menziesii* (Mirb.) Franco) growth decrease in Western US forests (Restaino et al. 2016).

Projected air temperature increase (IPCC 2014) will lead to further Siberian pine and fir area reduction in the lowlands, and area increase in the highlands, as well as trees migration into the alpine tundra. Moreover, warming will also adversely affect wildfire regime; thus, both fire frequency and burned area in Siberia have increased in recent decades (Kharuk and Ponomarev 2017). An additional factor of tree mortality is an activation of primary pests such as Siberian silkmoth (*Dendrolimus sibiricus*), which extended its range northward and caused huge forest mortality (about 800 thousand ha) in the mid-taiga zone (Kharuk et al. 2017d).

15.5 Conclusions

1. Warming hiatus in the ASR caused a general increase in the EGC area (+20% mean). However, in the lowlands (<1000 m a.s.l.), the EGC area decreased (−7%) with significant (+30%) increase at high elevations (>1000 m). The EGC area increase in the highlands correlated with air temperature mainly. Tree mortality in the lowlands was caused by the increased water stress via elevated temperature in synergy with bark-beetles attacks.
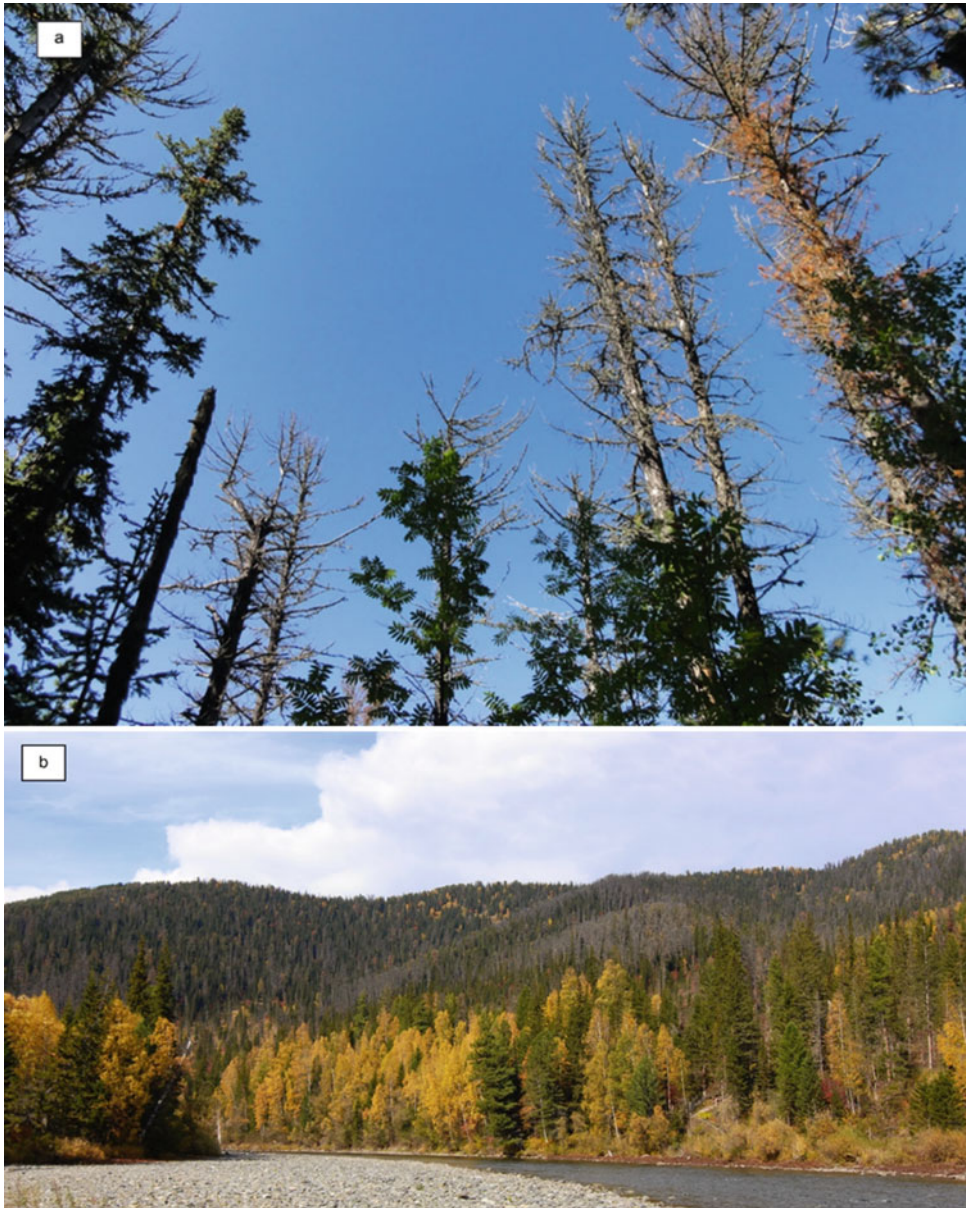
Fig. 15.10   Siberian pine trees **a** and stands **b** (gray color) mortality at middle elevations

Fig. 15.11 Old-growth Siberian pines in the refugium (c. 1900 m)

2. Elevated temperatures facilitated *Pinus sibirica* growth index (GI) since 1970s within all elevation belts. Within the zone of sufficient precipitation (highlands), the GI demonstrates permanent increase since warming onset. Meanwhile, within middle elevation belt (i.e., "Siberian pine—softwoods" transition), the GI curve has a breakpoint (c. 1983) with subsequent GI depression. After the breakpoint, the GI correlation switched from positive to negative with air temperature. Along with that, positive correlations between the GI and "moisture parameters" (precipitation, RZM, SPEI) have arisen.

3. Within the alpine forest–tundra ecotone, warming leads to transformation of prostrate Siberian pine into the vertical form. Alongside air temperature, growth of Siberian pine was also limited by moistening.

4. Under the projected climate change scenario, Siberian pine will shrink its habitat at middle and low elevations with substitution by drought-resistant larch and softwoods species.
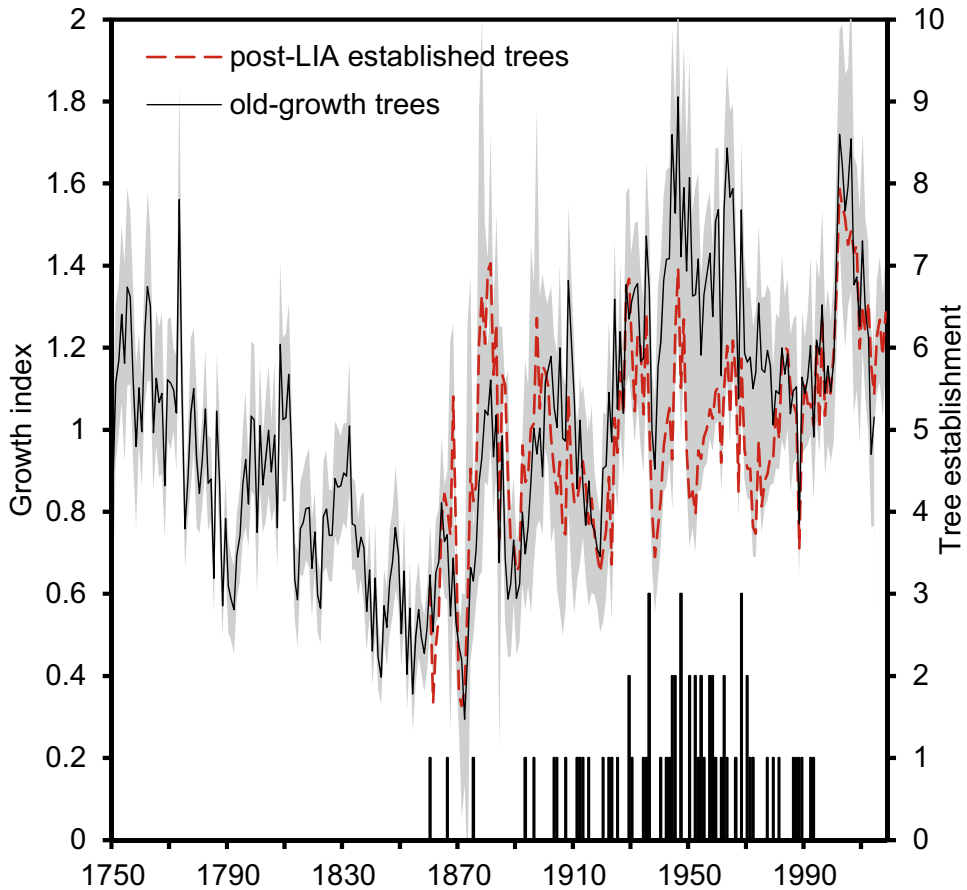
Fig. 15.12 GI dynamics of old-growth trees within the refugium (established before LIA; $N = 20$) and trees established since post-LIA warming ($N = 70$). Data of tree establishments indicated by *columns*

References

Allen CD, Macalady AK, Chenchouni H et al (2010) A global overview of drought and heat-induced tree mortality reveals emerging climate change risks for forests. For Ecol Manage 259(4):660–684. https://doi.org/10.1016/j.foreco.2009.09.001

Allen CD, Breshears DD, McDowell NG (2015) On underestimation of global vulnerability to tree mortality and forest die-off from hotter drought in the Anthropocene. Ecosphere 6(8):129. https://doi.org/10.1890/ES15-00203.1

Andregg LDL, Andregg WRL, Berry JA (2013) Not all droughts are created equal: translating meteorological drought into woody plant mortality. Tree Physiol Rev 33(7):701–712. https://doi.org/10.1093/treephys/tpt044

Cailleret M, Jansen S, Robert EMR et al (2017) A synthesis of radial growth patterns preceding tree mortality. Glob Change Biol 23(4):1675–1690. https://doi.org/10.1111/gcb.13535

Chuprov NP (2008) About the problem of spruce decay in the European North of Russia. Russ Forest 1:24–26 (in Russian)

Churakova SO, Saurer M, Bryukhanova MV et al (2016) Site-specific water-use strategies of mountain pine and larch to cope with recent climate change. Tree Physiol 36:942–953. https://doi.org/10.1093/treephys/tpw060

Coleman TW, Jones MI, Courtial B et al (2014) Impact of the first recorded outbreak of the Douglas-fir tussock moth, Orgyia pseudotsugata, in southern California

and the extent of its distribution in the Pacific Southwest region. For Ecol Manage 329:295–305. https://doi.org/10.1016/j.foreco.2014.06.027

Devi N, Hagedorn F, Moiseev P et al (2008) Expanding forests and changing growth forms of Siberian larch at the Polar Urals treeline during the 20th century. Glob Change Biol 14(7):1581–1591. https://doi.org/10.1111/j.1365-2486.2008.01583.x

Friedl MA, Sulla-Menashe D, Tan B et al (2010) MODIS Collection 5 global land cover: Algorithm refinements and characterization of new datasets. Remote Sens Environ 114:168–182. https://doi.org/10.1016/j.rse.2009.08.016

Gelaro R, McCarty W, Suárez MJ et al (2017) The modern-era retrospective analysis for research and applications, version 2 (MERRA-2). J Clim 30:5419–5454. https://doi.org/10.1175/JCLI-D-16-0758.1

Harris IC, Jones PD (2017) CRU TS4.01: University of East Anglia Climatic Research Unit; Climatic Research Unit (CRU) Time-Series (TS) version 4.01 of high-resolution gridded data of month-by-month variation in climate (Jan 1901–Dec 2016). Centre for Environmental Data Analysis, 04 Dec 2017. https://doi.org/10.5285/58a8802721c94c66ae45c3baa4d814d0

Hartmann DL, Klein Tank AMG, Rusticucci M et al (2013) Observations: atmosphere and Surface. In: Stocker TF, Qin D et al (eds) Climate change 2013: the physical science basis. Contribution of working group I to the fifth assessment report of the intergovernmental panel on climate change. Cambridge University Press, Cambridge, United Kingdom and New York, NY, USA

Haynes KJ, Allstadt A, Klimetzek D (2014) Forest defoliator outbreaks under climate change: effects on the frequency and severity of outbreaks of five pine insect pests. Global Change Biol 20:2004–2018. https://doi.org/10.1111/gcb.12506

He Y, Huang J, Shugart HH et al (2017) Unexpected evergreen expansion in the Siberian forest under warming hiatus. J Clim 30:5021–5039. https://doi.org/10.1175/JCLI-D-16-0196.1

Holmes RL (1983) Computer-assisted quality control in tree-ring dating and measurement. Tree-Ring Bull 43:69–78

Hogg EH, Michaelian M, Hook TI, Undershultz ME (2017) Recent climatic drying leads to age-independent growth reductions of white spruce stands in western Canada. Glob Change Biol 23(12):5297–5308. https://doi.org/10.1111/gcb.13795

IPCC (2014) Climate change 2014: impacts, adaptation, and vulnerability. In: Field CB, Barros VR et al (eds) A contribution of working group II to the fifth assessment report of the intergovernmental panel on climate change. World Meteorological Organization, Geneva, Switzerland, p 190. Available online: https://www.ipcc.ch/report/ar5/wg2/. Accessed on 19 May 2017

Kharuk VI, Ponomarev EI (2017) Spatiotemporal characterisics of wildfire frequency and relative area burned in larch-dominated forests of Central Siberia. Russ J Ecol 48(6):507–512

Kharuk VI, Dvinskaya ML, Ranson KJ, Im ST (2005) Expansion of evergreen conifers to the larch-dominated zone and climatic trends. Russ J Ecol 36(3):164–170. https://doi.org/10.1007/s11184-005-0055-5

Kharuk VI, Ranson KJ, Im ST, Vdovin AS (2010) Spatial distribution and temporal dynamics of high-elevation forest stands in southern Siberia. Glob Ecol Biogeogr 19:822–830. https://doi.org/10.1111/j.1466-8238.2010.00555.x

Kharuk VI, Im ST, Oskorbin PA et al (2013) Siberian pine decline and mortality in southern Siberian Mountains. For Ecol Manage 310:312–320. https://doi.org/10.1016/j.foreco.2013.08.042

Kharuk VI, Ranson KJ, Oskorbin PA, Im ST, Dvinskaya ML (2013) Climate induced birch mortality in Trans-Baikal lake region, Siberia. For Ecol Manage 289:385–392. https://doi.org/10.1016/j.foreco.2012.10.024

Kharuk VI, Im ST, Dvinskaya ML et al (2015) Climate-induced mortality of spruce stands in Belarus. Environ Res Lett 10:125006. https://doi.org/10.1088/1748-9326/10/12/125006

Kharuk VI, Demidko DA, Fedotova EV et al (2016) Spatial and temporal dynamics of Siberian silk moth large-scale outbreak in dark-needle coniferous tree stands in Altai. Contemp Probl Ecol 9:711–720. https://doi.org/10.1134/S199542551606007X

Kharuk VI, Im ST, Dvinskaya ML et al (2017a) Tree wave migration across an elevation gradient in the Altai Mountains. J Mt Sci 14(3):442–452. https://doi.org/10.1007/s11629-016-4286-7

Kharuk VI, Im ST, Petrov IA et al (2017b) Fir decline and mortality in the southern Siberian Mountains. Reg Environ Change 17:803–812. https://doi.org/10.1007/s10113-016-1073-5

Kharuk VI, Im ST, Petrov IA et al (2017c) Climate-induced mortality of Siberian pine and fir in the Lake Baikal Watershed, Siberia. For Ecol Manage 384:191–199. https://doi.org/10.1016/j.foreco.2016.10.050

Kharuk VI, Im ST, Ranson KJ, Yagunov MN (2017d) Climate-induced northerly expansion of Siberian Silkmoth range. Forests 8(8):301. Available online: https://www.mdpi.com/1999-4907/8/8/301/pdf. Accessed on 5 June 2018. https://doi.org/10.3390/f8080301

Kharuk VI, Im ST, Petrov IA (2018) Warming hiatus and evergreen conifers in Altay-Sayan Region, Siberia. J Mountain Sci 15(12):2579–2589. https://doi.org/10.1007/s11629-018-5071-6 10.1007/s11629-016-4286-7

Kolb TE, Fettig CJ, Ayres MP et al (2016) Observed and anticipated impacts of drought on forests insects and diseases in the United States. For Ecol Manage 380:321–324. https://doi.org/10.1016/j.foreco.2016.04.051

Krivecz SA, Kerchev IA, Bisirova EM et al (2015) Expansion of four-eyed fir bark beetle Polygraphus proximus blandf. (coleoptera, curculionidae: colytinae) in Siberia. Issues Saint-Petersburg For Tech Acad 211:33–45 (in Russian)

Luferov AO, Kovalishin VR (2017) Problem of mortality of pine stands on the territory of Belarus and Ukraine woodlands. Materials of the fifth international conference-meeting "Preservation of forest genetic resources". 2–7 Oct 2017, Gomel, Belarus. Belarus Institute of forest NAN, "Kolordryg" publishing. pp 119–120. (in Russian)

Man'ko YI, Gladkova GA, Butovets GN, Norihiza Kamibayasi (1998) Monitoring of fir-spruce forests decay in the Central Sikhote-Alin. Russ For Sci 1:3–16. (in Russian)

Medhaug I, Stolpe MB, Fischer EM, Knutti R (2017) Reconciling controversies about the global warming hiatus. Nature 545:41–47. https://doi.org/10.1038/nature22315

Michaelian M, Hogg EH, Hall RJ, Arsenault E (2011) Massive mortality of aspen following severe drought along the southern edge of the Canadian boreal forest. Global Change Biol 17(6):2084–2094. https://doi.org/10.1111/j.1365-2486.2010.02357.x

Millar CI, Stephenson NL (2015) Temperate forest health in an era of emerging megadisturbance. Science 349 (6250):823–826. https://doi.org/10.1126/science.aaa9933

Petrov IA, Kharuk VI, Dvinskaya ML, Im ST (2015) Reaction of coniferous trees in the Kuznetsk Alatau Alpine Forest-Tundra Ecotone to climate change. Contemp Probl Ecol 8(4):423–430. https://doi.org/10.1134/S1995425515040137

Restaino CM, Peterson DL, Littell J (2016) Increased water deficit decreases Douglas fir growth throughout western US forests. Proc Natl Acad Sci 113(34):9557–9562. https://doi.org/10.1073/pnas.1602384113

Rinn F (1996) Tsap V 3.6. Reference manual: computer program for tree-ring analysis and presentation. Heidelberg, Germany

Rossi S, Deslauriers A, Griçar J et al (2008) Critical temperatures for xylogenesis in conifers of cold climates. Glob Ecol Biogeogr 17:696–707. https://doi.org/10.1111/j.1466-8238.2008.00417.x

Sarnatczkii VV (2012) Zonal-typological patterns of periodic large-scale spruce decay in Belarus. In: Proceedings of BGTU. Forest estate, pp 274–276. (in Russian)

Shen ZQ, Lu J, Hua M, Fang JP (2016) Spatial pattern analysis and associations of different growth stages of populations of Abies georgei var. smithii in Southeast Tibet, China. J Mt Sci 13(12):2170–2181. https://doi.org/10.1007/s11629-016-3849-y

Speer JH (2010) Fundamentals of tree-ring research. University of Arizona Press, p 368

Vicente-Serrano SM, Beguería S, López-Moreno JI (2010) A multi-scalar drought index sensitive to global warming: the standardized precipitation evapotranspiration index—SPEI. J Clim 23:1696–1718. https://doi.org/10.1175/2009JCLI2909.1

Wong MHG, Duan CQ, Long YC, Luo Y, Xie GQ (2010) How will the distribution and size of subalpine Abies georgei forest respond to climate change? A study in Northwest Yunnan, China. Phys Geography 31 (4):319–335. https://doi.org/10.2747/0272-3646.31.4.319